Half-quantized Non-Abelian Vortices in Neutron $^3P_2$ Superfluids inside Magnetars

Kota Masuda[1,2] and Muneto Nitta[3*]
[1] *Department of Physics, The University of Tokyo, Tokyo 113-0033, Japan*
[2] *Theoretical Research Division, Nishina Center, RIKEN, Wako 351-0198, Japan*
[3] *Department of Physics at Hiyoshi, and Research and Education Center for Natural Sciences, Keio University, Hiyoshi 4-1-1, Yokohama, Kanagawa 223-8521, Japan*
(Dated: February 24, 2016)

We point out that half-quantized non-Abelian vortices exist as the minimum energy states in rotating neutron $^3P_2$ superfluids in the inner cores of magnetars with magnetic field greater than 3×10^{15} Gauss, while they do not in ordinary neutron stars with smaller magnetic fields. One integer vortex is split into two half-quantized vortices. The number of vortices is about 10^{19} and they are separated at about μm in a vortex lattice for typical parameters, while the vortex core size is about 10-100 fm. They are non-Abelian vortices characterized by non-Abelian first homotopy group, and consequently when two vortices corresponding to non-commutative elements collide, a rung vortex must be created between them, implying the formation of an entangled vortex network inside the cores of magnetars. We find the spontaneous magnetization in the vortex core showing anti-ferromagnetism whose typical magnitude is about 10^{8-9} Gauss that is ten times larger than that of integer vortices, when external magnetic fields are present along the vortex line.

arXiv:1602.07050v1 [nucl-th] 23 Feb 2016

I. INTRODUCTION

Neutron stars (NSs) or pulsars are rapidly rotating, massive and compact stars accompanied by a strong magnetic field, and so they provide a subject extensively studied in broad area of physics from astrophysics to nuclear and high energy physics and condensed matter physics. Most abundant middle-aged pulsars show magnetic field $B \sim 10^{11-13}$ Gauss on their surfaces. In recent years, young NSs with much stronger magnetic field $B \sim 10^{13-15}$ Gauss on their surfaces have been observed by the observations of some soft gamma ray repeaters and anomalous X-ray pulsars. This class of NSs is called as magnetars [1–4]. There have been various theoretical attempts to attribute the origin of the strong magnetic field of NSs to the intrinsic magnetization of the neutron star matter. However, no enough explanation about their origin has been given. Here, we discuss consequences of such strong magnetic fields in magnetars in the presence of neutron superfluids in their cores.

Neutrons are believed to form Cooper pairs to constitute a superfluid inside the cores of neutron stars since the proposal [5], as in liquid helium 3, metallic superconductors, and ultracold fermion gases. At densities lower than the normal nuclear matter density, the conventional and isotropic singlet ($^1S_0$) pairs are formed while the anisotropic triplet ($^3P_2$) attractive interaction becomes comparable to the $^1S_0$ pairs at the normal nuclear matter density, where a transition is expected to occur [6–11]. The widely accepted observational evidence for the existence of neutron superfluids is observed long relaxation time τ ($\sim$ weeks for Crab and $\sim$ years for Vela) after pulser glitches [12–14]. Other signals contain the sudden speed-up events of neutron stars (called pulsar glitches [15]) proposed to be a consequence of the unpinning dynamics of a large number of superfluid vortices pinned on the nuclei [16], and the cooling process of a neutron star [17, 18]. One of the most important consequences of the existence of a superfluid would be superfluid vortices. If a superfluid is rotating inside a neutron star, it must be threaded by superfluid vortices along the rotation axis, as well established in helium superfluids and ultracold atomic gases. The number N_v of vortices with the unit circulation created inside rotating neutron stars can be estimated to be

$$N_v \sim 1.9 \times 10^{19} \left(\frac{1\text{ms}}{P}\right) \left(\frac{M^*}{900\text{MeV}}\right) \left(\frac{R}{10\text{km}}\right)^2 \quad (1)$$

using the period P of the neutron star, the effective neutron mass M^* , and the radius R of the neutron superfluid. The vortices will constitute a lattice, and the mean distance between vortices is about $d \sim 1.7 \times 10^{-6}$m for the typical values for P, M^* and R in Eq. (1), which is much larger than the coherence length $\xi \sim 10 - 100$ fm of the neutron superfluid, or the core size of vortices. Therefore, a large number of thin vortices must exist.

Exotic vortices are predicted to exist in recent developments of ultracold atomic gases, in particular in spinor Bose-Einstein condensates (BECs). Prime examples are fractionally quantized non-Abelian vortices [19–21] in spin-2 BECs. The term "non-Abelian" indicates elements of the first homotopy group to be non-Abelian (non-commutative) [22, 23], and consequently when two non-Abelian vortices, characterized by homotopy group elements that do not commute, collide, it is inevitable to form a rung vortex that bridges the two vortices [20, 22, 23], implying the formation of a tangled network of vortices and long lifetime of vortices after their formation at the phase transition [24–26]. Such non-Abelian vortices may drastically change statistical properties of superfluids in non-equilibrium, such as the Kolmogorov law of energy cascades of quantum turbulence.

* masuda(at)nt.phys.s.u-tokyo.ac.jp, nitta(at)phys-h.keio.ac.jp

In this Letter, we point out that such non-Abelian vortices are present stably instead of conventional vortices in the neutron $^3P_2$ superfluids in the cores of neutron stars when they are accompanied by strong magnetic field larger than 3×10^{15} Gauss corresponding to magnetars. In order to study the $^3P_2$ superfluids, the Ginzburg-Landau (GL) free energy, derived in Refs. [10, 11] in the weak coupling limit, is useful although it is valid only near the critical temperature. For instance, the ground state was determined to be in the nematic phase [27] according to the classification by Mermin [28]. In the absence of magnetic field, it is continuously degenerated up to the forth order, as the nematic phase of spin-2 BECs [29, 30]. The ground state in the presence of the magnetic field has been determined recently [31] to be the uniaxial nematic phase with the magnetic field smaller than 10^{14} Gauss corresponding to ordinary neutron stars, the D_2 biaxial nematic with intermediate magnetic field, and the D_4 biaxial nematic phase with magnetic field stronger than 3×10^{15} Gauss corresponding to magnetars. Integer vortex structures in $^3P_2$ superfluids were discussed in the GL equation in the absence [11, 32, 33] and the presence [31] of magnetic fields. In particular, the spontaneous magnetization of a vortex core, pointed out in Ref. [33], has been calculated explicitly [31]. Here, we find half-quantized non-Abelian vortices in the $^3P_2$ superfluids in magnetars. In this case, the ground state is in the D_4 biaxial nematic phase. An integer vortex studied before is unstable to decay into two half-quantized non-Abelian vortices, and therefore non-Abelian vortices are the most fundamental topological degrees of freedom. We classify vortices, construct the vortex solutions, and calculate the magnetization of the vortex core induced by the neutron anomalous magnetic moment, with finding that it behaves as an anti-ferromagnet; it is magnetized opposite to the direction of the applied magnetic field. The typical magnitude of the magnetic field inside the vortex core is about 10^{7-8} Gauss that is ten times larger than that of integer vortices.

II. GINZBURG LANDAU FREE ENERGY FOR $^3P_2$ SUPERFLUIDS AND THE GROUND STATE

We first give the GL free energy and determine the ground states in the presence of strong magnetic fields. The GL free energy for the $^3P_2$ superfluids was derived in Refs. [10, 11, 34] in the weak coupling limit by considering only the excitations around the Fermi surface and assuming the contact interaction. The order parameter for $^3P_2$ superfluidity is given by 3×3 traceless symmetric tensor $A_{\mu i}$ defined by

$$\Delta=\sum_{\mu i} i\sigma_\mu\sigma_y A_{\mu i}k_i \tag{2}$$

with the gap parameter Δ. Here, the Latin letter μ and the Roman letter i stand for the spin index and spatial coordinates, respectively. The continuous symmetry acting on the matrix A is

$$A\to e^{i\theta}gAg^T,\quad e^{i\theta}\in U(1),\quad g\in SO(3). \tag{3}$$

The free energy density F can be written as

$$F=\int d^3\rho\ (f_{\rm grad}+f_{2+4}+f_6+f_H) \tag{4}$$

where the gradient term $f_{\rm grad}$, the second, fourth f_{2+4} and sixth order f_6 terms [34] and the magnetic interaction term f_H are given by

$$\begin{aligned}
f_{\rm grad}&=K_1\partial_iA_{\mu j}\partial_iA^\dagger_{\mu j}+K_2(\partial_iA_{\mu i}\partial_jA^\dagger_{\mu j}+\partial_iA_{\mu j}\partial_jA^\dagger_{\mu i})\\
f_{2+4}&=\alpha{\rm Tr}AA^\dagger+\beta[({\rm Tr}AA^\dagger)^2-{\rm Tr}A^2A^{\dagger2}],\\
f_6&=\gamma[-3({\rm Tr}AA^\dagger)|{\rm Tr}AA|^2+4({\rm Tr}AA^\dagger)^3\\
&\quad+12({\rm Tr}AA^\dagger){\rm Tr}(AA^\dagger)^2+6({\rm Tr}AA^\dagger){\rm Tr}(A^2A^{\dagger2})\\
&\quad+8{\rm Tr}(AA^\dagger)^3+12{\rm Tr}[(AA^\dagger)^2A^\dagger A]\\
&\quad-12{\rm Tr}[AA^\dagger A^\dagger A^\dagger AA]-12{\rm Tr}AA({\rm Tr}AA^\dagger AA)^*],\\
f_H&=g'_HH^2{\rm Tr}(AA^\dagger)+g_HH_\mu(AA^\dagger)_{\mu\nu}H_\nu,
\end{aligned} \tag{5}$$

respectively. The GL parameters are summarized in Appendix A.

Following the classification of the ground states in the general case [28], the ground state of $^3P_2$ superfluids was found to be in the nematic phase [27], in which the tensor A is in the form of $A\propto{\rm diag}(r,-(1+r),1)$ with a real parameter $r\in\mathbb{R}$ $(-1\le r\le-1/2)$. The ground state in the presence of external magnetic field H was determined recently [31] to be in the UN phase ($r=-1/2$) or in D_2 BN phase ($-1<r<-1/2$) for the weak magnetic field for ordinary neutron stars, and the D_4 BN phase ($r=-1$) for the strong magnetic field greater than 3×10^{15} Gauss for magnetars. Here, we consider such strong magnetic fields along the vortex line in the z direction ($\boldsymbol{H}\parallel\boldsymbol{z}$) or the angular direction ($\boldsymbol{H}\parallel\boldsymbol{\theta}$). In the ground state, the eigenvalues of the matrix A are 1, -1 and 0, among which the zero eigenvalue is directed along the magnetic field so that the energy contribution from the magnetic fields vanish. Consequently, the order parameter

$$A_{\rm g.s.}=\pm\sqrt{|\alpha|/2\beta}\,{\rm diag.}\,(1,-1,0) \tag{6}$$

is diagonalized in the (x,y,z) coordinate basis for $\boldsymbol{H}\parallel\boldsymbol{z}$ and in the (ρ,z,θ) basis for $\boldsymbol{H}\parallel\boldsymbol{\theta}$. For the latter case, non-zero components are $A_{\rho\rho}=-A_{zz}=\pm\sqrt{|\alpha|/2\beta}$, and the order parameter in the original Cartesian (x,z,y) coordinate basis can be obtained by $O(\theta)A_{\rm g.s.}O^T(\theta)$ with

$$O(\theta)=\begin{pmatrix}\cos\theta&0&-\sin\theta\\0&1&0\\\sin\theta&0&\cos\theta\end{pmatrix}. \tag{7}$$

The symmetry of this state is D_4 defined by

$$\begin{aligned}
&D_4=\{(1,\mathbf{1}_3),(1,I_1),(1,I_2),(1,I_3),(-1,R),\\
&\quad(-1,I_1R),(-1,I_2R),(-1,I_3R)\}\subset U(1)\times SO(3),\\
&I_1=\begin{pmatrix}1&&\\&-1&\\&&-1\end{pmatrix}\quad I_2=\begin{pmatrix}-1&&\\&1&\\&&-1\end{pmatrix},\\
&I_3=\begin{pmatrix}-1&&\\&-1&\\&&1\end{pmatrix},\quad R=\begin{pmatrix}0&-1&\\1&0&\\&&1\end{pmatrix}.
\end{aligned} \tag{8}$$

Here, $I_{1,2,3}$ represent for π rotations around the first, second and third axes, respectively, where the labels represent for $(1,2,3)=(x,y,z)$ for $\boldsymbol{H}\parallel\boldsymbol{z}$ and $(1,2,3)=(\rho,z,\theta)$ for $\boldsymbol{H}\parallel\boldsymbol{\theta}$. The element R represents for $\pi/2$ rotation around the the third (z or θ)-axis ($R^2=I_3$) and is accompanied by a π phase rotation of $U(1)$. The same D_4 BN phase appears in spin-2 BECs [21, 29, 30], and so these systems share common features. The order parameter space (OPS) of the D_4 BN phase is

$$G/H=\frac{U(1)\times SO(3)}{D_4}\simeq\frac{U(1)\times SU(2)}{D_4^*} \tag{9}$$

where D_4^* is the universal covering group of D_4, given by

$$\begin{aligned}D_4^*=\{&(1,\pm\mathbf{1}_2),(1,\pm i\sigma_1),(1,\pm i\sigma_2),(1,\pm i\sigma_3),\\ &(-1,\pm C),(-1,\pm i\sigma_1 C),(-1,\pm i\sigma_2 C),(-1,\pm i\sigma_3 C)\},\\ C=\frac{1}{\sqrt{2}}&\begin{pmatrix}1+i & 0\\ 0 & 1-i\end{pmatrix},\quad (C^2=i\sigma_3)\end{aligned} \tag{10}$$

with the Pauli matrices σ_a. The nontrivial homotopy groups of the OPS in Eq. (9) up to the 4th are

$$\pi_1=\mathbb{Z}\times_h D_4^*,\quad \pi_3=\mathbb{Z},\quad \pi_4=\mathbb{Z}_2. \tag{11}$$

We focus on the first homotopy group characterizing vortices, that contains non-Abelian group D_4^* (see Ref. [35] for the definition of the product "$\times_h$"). The first four elements constitute the quaternion group $\mathbb{Q}$ for spin vortices in biaxial nematic liquid [23, 36, 37], while the rests correspond to half-quantized non-Abelian vortices. We note that when two vortices characterized by the elements a and b collide, a vortex characterized by $[a,b]$ is created when it is a nonzero element and bridges these two vortices [23].

III. HALF-QUANTIZED VORTEX

Here we construct a half-quantized vortex corresponding to $(-1,R)$ in Eq. (8) and $(-1,\pm C)$ in Eq. (10). We consider the following Ansatz for the order parameter of a vortex state

$$\begin{aligned}A=\sqrt{\frac{|\alpha|}{6\beta}}e^{i\theta/2}R(\theta)&\begin{pmatrix}f & ige^{im\theta+i\delta} & 0\\ ige^{im\theta+i\delta} & -f & 0\\ 0 & 0 & 0\end{pmatrix}R^T(\theta)\\ R(\theta)=&\begin{pmatrix}\cos\theta/4 & -\sin\theta/4 & 0\\ \sin\theta/4 & \cos\theta/4 & 0\\ 0 & 0 & 1\end{pmatrix},\end{aligned} \tag{12}$$

in the (x,y,z) basis for $\boldsymbol{H}\parallel\boldsymbol{z}$ and in the (ρ,z,θ) basis for $\boldsymbol{H}\parallel\boldsymbol{\theta}$, with the position dependence in the cylindrical coordinates (ρ,θ,z). For the latter, the order parameters in the Cartesian (x,z,y) coordinates is $O(\theta)AO^T(\theta)$ with Eq. (7). Here m is an integer and $f(\rho),g(\rho)$ are profile functions with the boundary conditions

$$(f,g)\to(\sqrt{3},0)\text{ as }\rho\to\infty,\quad (0,0)\text{ as }\rho\to 0. \tag{13}$$

The configuration in Eq. (12) corresponds to the element $(-1,R)$ of π_1 in Eq. (10) because of $R(\theta)=R$ and $e^{i\theta/2}=-1$ at $\theta=2\pi$. The overall phase $e^{i\theta/2}$ represent half-quantization. Although $e^{i\theta/2}$ is not single-valued, R gives the minus sign with keeping the order parameter itself single-valued at $\theta=2\pi$. The Ansatz in Eq. (12) is the most general for axially symmetric configurations where the other components must vanish to be compatible with the group action.

We now solve vortex solutions numerically. With the boundary conditions in Eq. (13), we solve the vortex profiles f and g as functions of the radial coordinate ρ and plot in Fig. 1 (a) and (b), respectively. In numerical simulations, we have changed ρ $(0\le\rho<\infty)$ as $\tanh\rho$ $(0\le\tanh\rho<1)$, divided the domain of $\tanh\rho$ into 100 parts and solved the equations of motion in Appendix C simultaneously in the Newton's method. We set the magnetic field (arbitrary) larger than 3×10^{15} Gauss, for which the results do not depend on the value of the magnetic field. In Fig. 1 (a), we plot the profiles f with $m=0$ (the red curves) and $m\neq0$ (the black curves) in the upper (for $\boldsymbol{H}\parallel\boldsymbol{z}$) and lower (for $\boldsymbol{H}\parallel\boldsymbol{\theta}$) panels. For both the cases, as shown by the equation of motions for the cylindrical basis in Appendix C, Eq. (C2) is proportional to g for $m\neq0$. Due to the boundary conditions $g=0$ at $\rho=0,\infty$, only the trivial solution $g=0$ is allowed for $m\neq0$ where all $m\neq0$ give the identical solution. For $\boldsymbol{H}\parallel\boldsymbol{\theta}$ in the lower panels, the profiles f with $m=0$ (the red curve) and $m\neq0$ (the black curves) take different values although they are almost overlapped. In summary, we have obtained two solutions $g\neq0$ and $g=0$ for each case of $\boldsymbol{H}\parallel\boldsymbol{z}$ and $\boldsymbol{H}\parallel\boldsymbol{\theta}$. The solutions $g=0$ are metastable solutions.

Next, we calculate the spontaneous magnetization of ${}^3P_2$ vortex cores due to the neutron anomalous magnetic moment. The vortex magnetization $\boldsymbol{M}(\rho)$ in the half-quantized vortex core can be calculated as

$$\boldsymbol{M}=\frac{\gamma_n\hbar}{2}\hat{\boldsymbol{\sigma}}, \tag{14}$$

with the gyromagnetic ratio γ_n of the neutrons and

$$\begin{aligned}\hat{\boldsymbol{\sigma}}&=T\sum_n\int\frac{d^3k}{(2\pi)^3}\mathrm{Tr}(\boldsymbol{\sigma}G(k,\omega_n))\\ &=\frac{4}{9}N'(0)k_F^2\frac{|\alpha|}{6\beta}g(\rho)2f(\rho)\cos m\theta\hat{\boldsymbol{z}}\end{aligned} \tag{15}$$

where $G(k,\omega_n)$ is a thermal Green function and $\omega_n=(2n+1)\pi T$ is the Matsubara frequency and $N'(0)=\frac{M^2}{2\pi^2k_F}$ is the density of states differentiated by the energy $E=k^2/2M$, $N'=\frac{M^2}{2\pi^2k}$, evaluated at the Fermi surface $k=k_F$. We obtain the magnetization $\boldsymbol{M}$ as a function of ρ and plot M_z in Fig. 1 (c). The red and black curves correspond to the cases for $g\neq0$ $(m=0)$ and $g=0$ $(m\neq0)$. First, due to the axial symmetry around the z axis, the (ρ,θ) component of the tensor $A_{\mu i}$ in the cylindrical basis or (x,y) component of the tensor $A_{\mu i}$ in the Cartesian basis must have the nonzero value to produce a net spontaneous magnetization along the z-axis. In the case with $\boldsymbol{H}\parallel\boldsymbol{\theta}$, the (ρ,θ) component of the tensor A is zero as shown in Eq. (12). Therefore, we obtain $M_z=0$ for all the cases. On the other

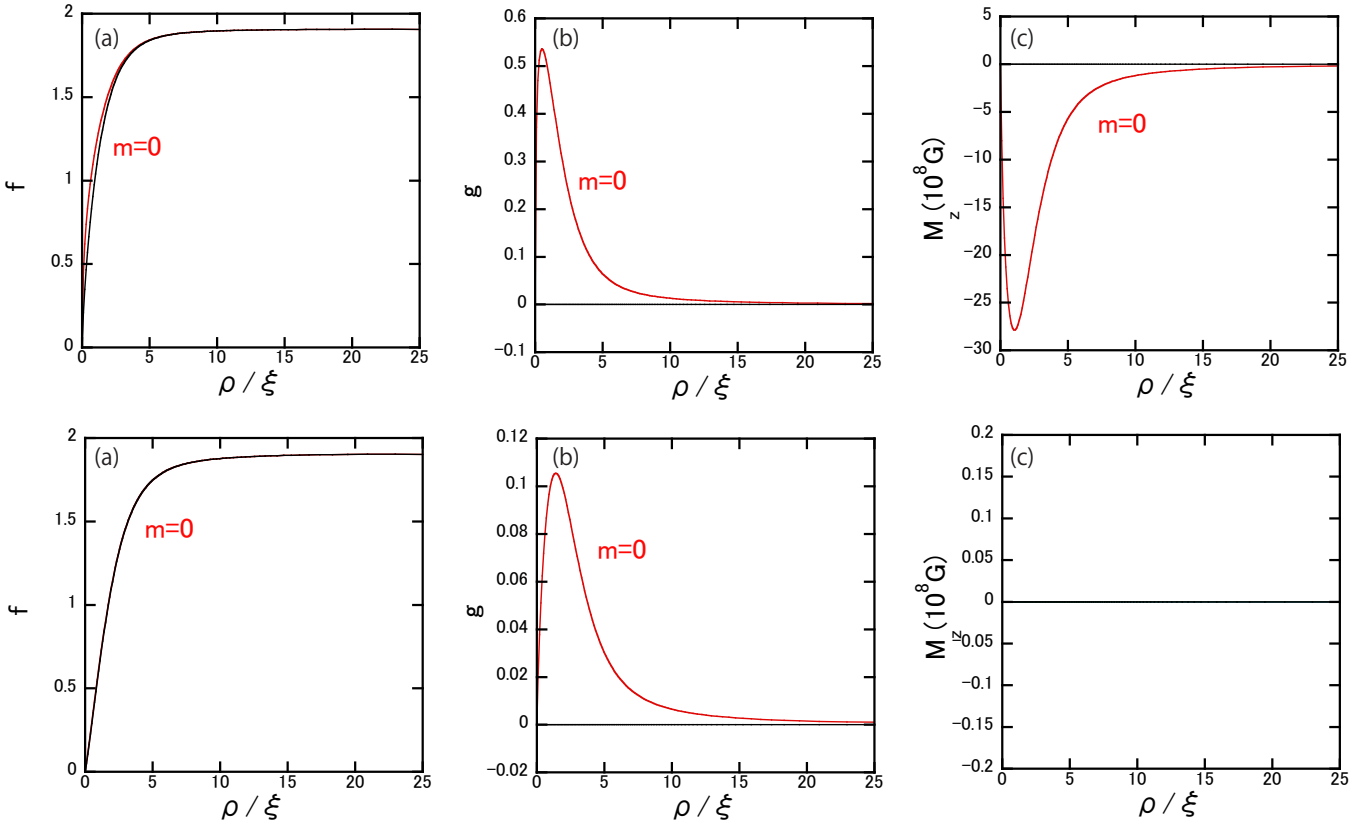

FIG. 1. The profile functions and the magnetization. The upper and lower panels are for $\boldsymbol{H} \parallel \boldsymbol{z}$ and $\boldsymbol{H} \parallel \boldsymbol{\theta}$, respectively. The profile functions (a) f and (b) g as functions of the distance ρ/ξ from the vortex center. The red and black curves correspond to $g \neq 0$ ($m = 0$) and $g = 0$ ($m \neq 0$) for which all m result in the same solution. (c) The dependence of the magnetizations M_z on the distance ρ/ξ from the vortex core.

hand, if we apply the magnetic field along the z-axis, the (x, y) component of the tensor A is proportional to g. As we already discussed, g has the nonzero value only for $m = 0$. This is the reason why only the case for $m = 0$ has the spontaneous magnetization. We have found that vortex core magnetization is anti-ferromagnetic, that is, the magnetization is anti-parallel to the direction of the external magnetic field. The maximum value of M_z is about 10^9 Gauss, that is ten times larger than that with the integer vortex [31]. This spontaneous magnetization is still negligible in observations, since the distance between vortices is much smaller than the coherence length as we discussed in Ref. [31] for the case of an integer vortex.

Finally, we discuss that half-quantized vortex states give the minimum energy in the D_4 BN phase under rotation rather than integer vortex states. For simplicity we concentrate on the case of $\boldsymbol{H} \parallel \boldsymbol{z}$. Fig. 2 shows how an integer vortex is split into two half-quantized vortices. Let us consider an integer vortex located at the origin, given by $e^{i\theta} A_{\rm g.s.}$ with Eq. (6) at large distance $\rho \to \infty$ encircled by a path $b_1 + b_2$. Along each of the paths b_1 and b_2, the overall phase of the gap is rotated by π. Now let us consider a path r along the x coordinate that splits $b_1 + b_2$. The integer vortex can be split into two

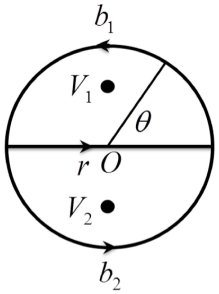

FIG. 2. Splitting an integer vortex into two half-quantized vortices.

half-quantized vortices separated in the y direction at V_1 and V_2. Along the path r, the tensor is given by $A = R(x) A_{\rm g.s.} R^T(x)$ where we assign an $SO(3)$ rotation $R(x)$ by $\pi/2$ given by

$$R(x) = \begin{pmatrix} \cos\alpha(x) & -\sin\alpha(x) & 0 \\ \sin\alpha(x) & \cos\alpha(x) & 0 \\ 0 & 0 & 1 \end{pmatrix}, \qquad (16)$$

with a real function $\alpha(x)$ satisfying the boundary conditions $\alpha(x) \to 0$ at $x \to -\infty$ and $\alpha(x) \to \pi/2$ at $x \to +\infty$. The closed paths $b_1 + r$ and $b_2 - r$ encircling V_1 and V_2, respectively, represent half-quantized vortices correspond-

ing to $(-1, R)$ and $(-1, RI_3) = (-1, -R)$, respectively in Eq. (10). When one of them is well separated from the other, it gives the configuration in Eq. (12) where both the phase and $SO(3)$ rotation become monotonic to decrease the energy. This splitting is energetically favored because the tension of the vortex is proportional to the circulation [the $U(1)$ winding number] squared. If the two half-quantized vortices are infinitely separated the energy is proportional to $(1/2)^2 + (1/2)^2 = 1/2$ that is less than 1 for one integer vortex.

IV. SUMMARY AND DISCUSSION

In summary, half-quantized non-Abelian vortices exist as the minimum energy configurations in rotating neutron $^3P_2$ superfluids in the inner cores of magnetars, in which the D_4 BN phase is realized. These vortices are superfluid vortices carrying half-quantized circulations and about 10^{19} vortices are created along the rotation axis for typical magnetars. When the magnetic field is present along the vortex line, the spontaneous magnetization occurs in the vortex core, exhibiting anti-ferromagnetism of the order 10^{8-9} Gauss that is ten times larger than that of integer vortices. It does not occur for magnetic field encircling the vortex line. These voritces belong to non-Abelian elements of the homotopy group π_1 and consequently a bridge must be created between them when they collide. Therefore the existence of an entangled network of vortices is predicted, implying long life time of vortices created at the phase transition. When the magnetic field is weaker than 10^{15} Gauss for ordinary neutron stars, the phase is in the D_2 or UN phase where half-quantized non-Abelian vortices do not exist. The existence and absence of non-Abelian vortices may characterize the distinct dynamics of magnetars and ordinary neutron stars. The nematic phase, including D_4 and D_2 BN and UN phases, also exists in spin-2 BECs of ultracold atomic gases, in which case these sub-phases are controllable experimentally, and so this opens a possibility to test certain aspects of physics of neutron stars in laboratory experiments.

ACKNOWLEDGMENTS

We thank Takeshi Mizushima for helpful discussions. KM thanks Mark Alford for the kind hospitality and discussions in Washington University in St. Louis where part of this work was carried out under the support of ALPS Program, University of Tokyo. KM is supported by JSPS Research Fellowship for Young Scientists. The work of M. N. is supported in part by a Grant-in-Aid for Scientific Research on Innovative Areas "Topological Materials Science" (KAKENHI Grant No. 15H05855) and "Nuclear Matter in Neutron Stars Investigated by Experiments and Astronomical Observations" (KAKENHI Grant No. 15H00841) from the the Ministry of Education, Culture, Sports, Science (MEXT) of Japan. The work of M. N. is also supported in part by the Japan Society for the Promotion of Science (JSPS) Grant-in-Aid for Scientific Research (KAKENHI Grant No. 25400268) and by the MEXT-Supported Program for the Strategic Research Foundation at Private Universities "Topological Science" (Grant No. S1511006).

[1] B. Paczynski, Acta Astron. **42**, 145 (1992).
[2] C. Thompson and R. C. Duncan, mnras **275**, 255 (1995).
[3] C. Thompson and R. C. Duncan, The Astrophysical Journal **473**, 322 (1996).
[4] A. Melatos, Astrophys. J. **519**, L77 (1999).
[5] A. B. Migdal, Nucl. Phys. **13**, 655 (1959).
[6] R. Tamagaki, Prog. Theor. Phys. **44**, 905 (1970).
[7] M. Hoffberg, A. E. Glassgold, R. W. Richardson, and M. Ruderman, Phys. Rev. Lett. **24**, 775 (1970).
[8] T. Takatsuka and R. Tamagaki, Prog. Theor. Phys. **46**, 114 (1971).
[9] T. Takatsuka, Prog. Theor. Phys. **47**, 1062 (1972).
[10] T. Fujita and T. Tsuneto, Prog. Theor. Phys. **48**, 766 (1972).
[11] R. W. Richardson, Phys. Rev. D **5**, 1883 (1972).
[12] G. Baym, C. J. Pethick, D. Pines, and M. Ruderman, Nature 224, 867 (1969).
[13] D. Pines, J. Shaham, and M. Ruderman, Nature, Phys. Sci. 237, 83 (1972).
[14] T. Takatsuka and R. Tamagaki, Prog. Theor. Phys. 79, 274 (1988).
[15] P. E. Reichley and G. S. Downs, Nature **234**, 48 (1971).
[16] P. W. Anderson and N. Itoh, Nature **256**, 25 (1975).
[17] C. O. Heinke and W. C. G. Ho, Astrophys. J. **719**, L167 (2010), arXiv:1007.4719 [astro-ph.HE].
[18] D. Page, M. Prakash, J. M. Lattimer, and A. W. Steiner, Phys. Rev. Lett. **106**, 081101 (2011), arXiv:1011.6142 [astro-ph.HE].
[19] G. W. Semenoff and F. Zhou, Phys. Rev. Lett. **98**, 100401 (2007), arXiv:cond-mat/0610162 [cond-mat].
[20] M. Kobayashi, Y. Kawaguchi, M. Nitta, and M. Ueda, Phys. Rev. Lett. **103**, 115301 (2009), arXiv:0810.5441 [cond-mat.other].
[21] Y. Kawaguchi and M. Ueda, Phys. Rept. **520**, 253 (2012).
[22] V. Poenaru and G. Toulouse, J. Phys. Lett. (Paris) **38**, 887 (1977).
[23] N. D. Mermin, Rev. Mod. Phys. **51**, 591 (1979).
[24] D. Spergel and U.-L. Pen, Astrophys. J. **491**, L67 (1997), arXiv:astro-ph/9611198 [astro-ph].
[25] P. McGraw, Phys. Rev. **D57**, 3317 (1998), arXiv:astro-ph/9706182 [astro-ph].
[26] M. Bucher and D. N. Spergel, Phys. Rev. **D60**, 043505 (1999), arXiv:astro-ph/9812022 [astro-ph].
[27] J. Sauls and J. Serene, Phys. Rev. D **17**, 1524 (1978).
[28] N. D. Mermin, Phys. Rev. **A9**, 868 (1974).
[29] J. L. Song, G. W. Semenoff, and F. Zhou, Phys. Rev. Lett. **98**, 160408 (2007), arXiv:cond-mat/0702052 [cond-mat.other].
[30] S. Uchino, M. Kobayashi, M. Nitta, and M. Ueda, Phys. Rev. Lett. **105**, 230406 (2010), arXiv:1010.2864 [cond-

mat.quant-gas].
[31] K. Masuda and M. Nitta, Phys. Rev. C (to appear) (2016), arXiv:1512.01946 [nucl-th].
[32] P. Muzikar, J. A. Sauls, and J. W. Serene, Phys. Rev. D **21**, 1494 (1980).
[33] J. A. Sauls, D. L. Stein, and J. W. Serene, Phys. Rev. D **25**, 967 (1982).
[34] J. A. Sauls, *Anisotropic Superfluidity in Neutron Stars and Strong Coupling Effect in Superfluid ^3He*, Ph.D. thesis, SUNY Stony Brook (1980).
[35] S. Kobayashi, M. Kobayashi, Y. Kawaguchi, M. Nitta, and M. Ueda, Nucl. Phys. **B856**, 577 (2012), arXiv:1110.1478 [math-ph].
[36] G. E. Volovik and V. P. Mineev, JETP **45**, 1186 (1977).
[37] J. Preskill and L. M. Krauss, Nucl. Phys. **B341**, 50 (1990).

Appendix A: GL parameters

In Table I, we summarize the coefficients (the GL parameters) of the GL free energy in Eq. (4), that are calculated in the weak coupling limit by considering only the excitations around the Fermi surface [10, 11, 34]. In this limit, K_1 and K_2 take the same value. In the derivation of α, we took $g = \frac{3\pi^2}{Mk_F^3}$ in order for the T dependence of α to become that of the BCS theory. k_F is the Fermi momentum defined by $k_F = \hbar c(3\pi^2\rho)^{1/3}$ with the neutron density ρ, $N(0) \equiv \frac{Mk_F}{2\pi^2}$ is the density of states $N = \frac{Mk}{2\pi^2}$ on the Fermi surface at $k = k_F$, T_c is the critical temperature for the $^3P_2$ superfluidity, γ_n is the gyromagnetic ratio of the neutrons and F is the Fermi liquid correction about the Pauli spin susceptibility.

The Riemann zeta function $\zeta(n)$ defined by $\zeta(n) = \sum_{k=1}^{\infty} \frac{1}{k^n}$ takes the values $\zeta(3) \sim 1.202$ and $\zeta(5) \sim 1.037$.

In this Letter, we have taken $F = -0.75$, $T_c = 0.2$MeV, $T = 0.8T_c$ and $\rho = 0.17/\text{fm}^3$ for numerical simulations.

Appendix B: The free energy of a vortex

We calculate the free energy per the unit length of a vortex in Eq. (12):

$$F = \int d^2\rho \, \frac{|\alpha|}{6\beta}\left(K_1 t_1 + K_2 t_2 + \alpha t_3 + \frac{|\alpha|}{6\beta}\beta t_4 + \frac{\alpha^2}{36\beta^2}\gamma t_5\right) \tag{B1}$$

where t_1 and t_2 are the gradient terms and, t_3, t_4 and t_5 are the second, fourth and sixth order terms, respectively in the GL free energy density in Eq. (4). Here $t_{1,2}$ can be written as

$$t_1^{(x,y,z)} = 2\left(f'^2 + g'^2\frac{\frac{1}{2}f^2 + \left(\frac{1}{4} + \left(m+\frac{1}{2}\right)^2\right)g^2}{\rho^2}\right) - \frac{2}{\rho^2}(m+1)fg\cos(m\theta+\delta), \tag{B2}$$

$$t_2^{(x,y,z)} = 2\left(f'^2 + g'^2\frac{\frac{1}{2}f^2 + \left(\frac{1}{4} + \left(m+\frac{1}{2}\right)^2\right)g^2}{\rho^2}\right) - \frac{2}{\rho^2}(m+1)fg\cos(m\theta+\delta) \tag{B3}$$

for the configurations diagonalized in the xyz basis, and

$$t_1^{(\rho,\theta,z)} = 2(f'^2+g'^2) + \frac{1}{\rho^2}\left(3f^2 + \left(\frac{5}{2} + 2\left(m+\frac{1}{2}\right)^2\right)g^2 - 2(m+1)fg\cos(m\theta+\delta)\right), \tag{B4}$$

$$t_2^{(\rho,\theta,z)} = 2(f'^2+g'^2) + \frac{2}{\rho}(ff'+gg') + \frac{2}{\rho^2}(f^2+g^2) \tag{B5}$$

for the configurations diagonalized in the cylindrical basis. The rest terms $t_{3,4,5}$ can be written in the both basis as

$$t_3 = 2(f^2+g^2), \tag{B6}$$

$$t_4 = 2f^4 + 2g^4 + 8f^2g^2 + 4f^2g^2\cos2(m\theta+\delta), \tag{B7}$$

$$t_5 = 48f^6 + 48g^6 + (432 + 288\cos2(m\theta+\delta))f^4g^2 + (432 + 288\cos2(m\theta+\delta))f^2g^4. \tag{B8}$$

We consider the case with $\delta = 0$ consistent with the equation of motion, in which the imaginary part of non-diagonal elements is directly coupled to the real part of diagonal element. However, the effect of δ is yet to be clarified.

By differentiating the total free energy with respect to f and g, we obtain the sets of the equation of motions for each basis, as summarized in Appendix C.

Appendix C: Equation of motion

Here, we write down the equation of motion explicitly in the cylindrical basis ($n = 1$) and xyz-basis ($n = 0$).

- The equation of motions for cylindrical basis ($n = 1$) are given as follows:

$$8\frac{\partial^2 f}{\partial\rho^2} + \frac{8}{\rho}\frac{\partial f}{\partial\rho} - \frac{1}{\rho^2}(10f - 2\delta_{m,0}g) + 4f - \frac{f}{6}\left(8f^2 + (16+8\delta_{m,0})g^2\right) - \frac{|\alpha|}{36\beta^2}\gamma\Big(288f^5 + g^2(1728+1152\delta_{m,0})f^3 + g^4(864+576\delta_{m,0})f\Big) = 0, \tag{C1}$$

α	$K_1 = K_2$	β	γ	g_H
$\frac{N(0)}{3}\frac{T-T_c}{T}k_F^2$	$\frac{7\zeta(3)}{240M^2}\frac{N(0)}{(\pi T_c)^2}k_F^4$	$\frac{7\zeta(3)}{60}\frac{N(0)}{(\pi T_c)^2}k_F^4$	$-\frac{31}{16}\frac{\zeta(5)}{840}\frac{N(0)}{(\pi T_c)^4}k_F^6$	$\frac{7\zeta(3)}{24}\frac{N(0)}{(\pi T_c)^2}\frac{(\gamma_n\hbar)^2}{2(1+F)^2}H^2k_F^2$

TABLE I. The GL parameters in the weak coupling limit.

$$8\frac{\partial^2 g}{\partial\rho^2}+\frac{8}{\rho}\frac{\partial g}{\partial\rho}-\frac{1}{\rho^2}\left(\left(9+4\left(m+\frac{1}{2}\right)^2\right)g-2\delta_{m,0}f\right)+4g-\frac{g}{6}\left(8g^2+(16+8\delta_{m,0})f^2\right)$$
$$-\frac{|\alpha|}{36\beta^2}\gamma\Big(288g^5+f^2(1728+1152\delta_{m,0})g^3+f^4(864+576\delta_{m,0})g\Big)=0. \tag{C2}$$

- The equation of motions for the xyz-basis ($n=0$) are given as follows:

$$8\frac{\partial^2 f}{\partial\rho^2}+\frac{8}{\rho}\frac{\partial f}{\partial\rho}-\frac{4}{\rho^2}\left(f-\delta_{m,0}g\right)+4f-\frac{f}{6}\left(8f^2+(16+8\delta_{m,0})g^2\right)$$
$$-\frac{|\alpha|}{36\beta^2}\gamma\Big(288f^5+g^2(1728+1152\delta_{m,0})f^3+g^4(864+576\delta_{m,0})f\Big)=0, \tag{C3}$$

$$8\frac{\partial^2 g}{\partial\rho^2}+\frac{8}{\rho}\frac{\partial g}{\partial\rho}-\frac{4}{\rho^2}\left(\left(\frac{1}{2}+2\left(m+\frac{1}{2}\right)^2\right)g-\delta_{m,0}f\right)+4g-\frac{g}{6}\left(8g^2+(16+8\delta_{m,0})f^2\right)$$
$$-\frac{|\alpha|}{36\beta^2}\gamma\Big(288g^5+f^2(1728+1152\delta_{m,0})g^3+f^4(864+576\delta_{m,0})g\Big)=0. \tag{C4}$$